International Journal of Ambient Energy

ISSN: (Print) (Online) Journal homepage: https://www.tandfonline.com/loi/taen20

Improved performance of polymer electrolyte membrane fuel cell using leaf-baffle flow field design

A'rasy Fahruddin, Djatmiko Ichsani, Fadlilatul Taufany, Budi Utomo Kukuh Widodo & Wawan Aries Widodo

To cite this article: A'rasy Fahruddin, Djatmiko Ichsani, Fadlilatul Taufany, Budi Utomo Kukuh Widodo & Wawan Aries Widodo (2022): Improved performance of polymer electrolyte membrane fuel cell using leaf-baffle flow field design, International Journal of Ambient Energy, DOI: 10.1080/01430750.2022.2037458

To link to this article: https://doi.org/10.1080/01430750.2022.2037458

Published online: 22 Feb 2022.

INTERNATIONAL JOURNAL OF AMBIENT ENERGY
https://doi.org/10.1080/01430750.2022.2037458

Check for updates

Improved performance of polymer electrolyte membrane fuel cell using leaf-baffle flow field design

A'rasy Fahruddin [a,b], Djatmiko Ichsani[a], Fadlilatul Taufany[c], Budi Utomo Kukuh Widodo[a] and Wawan Aries Widodo[a]

[a]Department of Mechanical Engineering, Institut Teknologi Sepuluh Nopember (ITS), Surabaya, Indonesia; [b]Department of Mechanical Engineering, Universitas Muhammadiyah Sidoarjo, Sidoarjo, Indonesia; [c]Department of Chemical Engineering, Institut Teknologi Sepuluh Nopember (ITS), Surabaya, Indonesia

ABSTRACT

The hydrogen fuel cell is an environmentally friendly alternative energy converter. Its performance is quite influenced by the geometry of the flow field. This study proposes a leaf-baffle flow field design with experimental testing compared to conventional models. Experiments were carried out on a single cell Polymer Electrolyte Membrane Fuel Cell with an active area of 25 cm^2, with flow field design variations of parallel, leaf, and leaf-baffle on the cathode. The performance of each design is compared with the polarisation and power density graphs, the pressure drop due to energy loss is also compared. The results showed that the leaf-baffle design produces the best performance, increased by 37.14% compared to parallels. Furthermore, to obtain better performance, the ratio of the reactants velocity to the branch length needs to be considered for designing the flow field.

ARTICLE HISTORY
Received 5 July 2021
Accepted 25 January 2022

KEYWORDS
Leaf baffle; flow field; fuel cell; velocity distribution; pressure drop

1. Introduction

Currently, liquid and gas fuel is still widely used because it is an effective and easy-to-distribute energy storage medium. However, renewable energy systems need to be developed to handle the problems associated with the depletion of fossil fuels and environmental issues that emerge due to combustion. Hydrogen is a clean and potential energy storage medium for the future because hydrogen can be easily formed from the electrolysis process utilising renewable energy or reformed from biofuel (Demirbas 2009; Liu 2019). A device for converting hydrogen into electricity is the fuel cell, which has greater efficiency and cleaner than ICE (Hosseini and Butler 2020; Lakshminarayanan and Karthikeyan 2020; Demirbas 2007). Furthermore, compared to conventional batteries of the same volume, mass, and charge time, fuel cell with hydrogen tank can store more energy (Bhatia and Riddell 2016; Velisala and Golagani 2020). However, they have certain disadvantages, such as expensiveness, and less efficient than the batteries (Stempien and Chan 2017). Therefore, it is still suitable for application on large vehicles such as buses, fork-lift, locomotive, and ships (Zhang, Zhang, and Xie 2020; Hosseinzadeh and Rokni 2013; Sarma and Ganguly 2018; Inal and Deniz 2020), as well as generators that are either used as backup or in remote areas (Cordiner et al. 2016), also lightweight aircraft and unmanned undersea vehicles (Arat et al. 2020; Lu et al. 2020).

Presently, several efforts are focused on developing a more efficient PEMFC that produces a high current density, thereby reducing fuel cells' prices while serving a life purpose. Numerous factors affect the performance of PEMFC, including issues associated with the distribution of reactants in the cell (Lim et al. 2016; Wang et al. 2011; Pan et al. 2020). The mal-distribution effect in its flow field is an important problem that needs to be considered because it leads to non-uniform current densities, performance drop, localised hot spots in the membrane, and material degradation. In conventional cells, parallel geometry is widely used for cathode reactant flow fields. Generally, maldistribution occurs due to non-uniform flow resistance in parallel channel (Manso et al. 2012).

Several studies have determined fuel cells' improved performance by adopting bio-inspired flow fields (Kloess et al. 2009; Badduri, Naga Srinivasulu, and Srinivasa Rao 2019). Roshandel, Arbabi, and Karimi Moghaddam (2012) carried out comparative research between a parallel, serpentine, and leaf bone design. The results showed that the leaf shape produces more uniform fuel and pressure distribution on catalyst surface, and produce higher power density than serpentine and parallel flow channels approximately 26% and 56%, respectively. Ozden (Ozden et al. 2017) researched the cathode channel's design on a Direct Methanol Fuel Cell by experiment. Four designs in the form of serpentine, lung shape, leaf shape I, and II were compared. Murray's law was applied to both leaf shapes to determine the width of the parent channel. The results from this study indicate that leaf shape II produces the best power density, which is relatively 88.8 mW/cm^2, while the serpentine channel generates 82.4 mW/cm^2. However, there is a possibility of increasing the distribution of reactants in PEMFC using the leaf flow field. According to the simulation results, there is usually a shortage of reactants at the branch's tips.

In addition to the uniform flow distribution, cell performance tends to be improved by increasing the force convection through the electrode. The addition of an obstacle to the channel can increase convective heat transfer, and this is proportional to the increase in mass transfer. This increases the oxygen

CONTACT A'rasy Fahruddin arasy.fahruddin@umsida.ac.id

Table 1. Properties of membrane electrolyte assembly.

Component	Properties
Membrane	Nafion NR-212; 50.8 µm
Anode and cathode catalyst	0.5 mg/cm^2; 60 wt% Pt, on Carbon Vulcan
Gas diffusion layer	Woven carbon fibre cloth; 0.410 mm

consumption in the catalyst layer as well as the performance of the fuel cell. Heidary et al. (2016) analysed the use of parallel flow fields as well as the addition of blockages on a cathode with in-line and staggered arrangements. The study results showed that this type of arrangement improves fuel cell performance from 10% to 28%.

The cathode flow field design is one factor that significantly influences the performance of the fuel cell. According to several studies, a good flow field design has the ability to enhance the velocity distribution of oxygen on the cathode, to enable it to meet the required reactant supply. Some studies have proven that leaf-inspired designs perform better than the parallel flow field. Hence, this study combines the use of baffles in the leaf flow field to further improve its performance experimentally.

2. Materials and methods

2.1. Experimental method

The experiments were carried out by generating a PEMFC single cell with MEA (Membrane Electrolyte Assembly) with a 25 cm^2 active area. MEA was ordered from FuelCellsEtc (fuelcellsetc.com) with the specifications shown in Table 1. In addition, the nine-layer fuel cell arrangement is shown in Figure 1. The copper plates are used as current collector, while both the anode and cathode are 3 mm thick. The flow field is made on a graphite plate with a thickness of 5 mm. Teflon gaskets and silicon paste are used to prevent the gas from leaking. For high currents, the electrical resistance is minimised. Clamp is used to reduce the contact resistance by pressing both plates at the end with similar pressure for each test.

The gas flow field design for anode side consists of a single serpentine in order to ensure that the hydrogen reacts completely. The flow of oxygen in the cathode is based on three comparable variations, in the form of parallel, leaf, and leaf-baffle, as shown in Figure 2. Branch channels in parallel and leaf flow fields were 1.25 mm wide (Fahruddin et al. 2019a), 1 mm deep. The baffle height in the branch channel of leaf-baffle flow field is 0.5 mm to obtain moderate pressure drop. Meanwhile, the baffles in the main channel increase in height towards the outlet channel so that the reactants flow towards the branches. Baffles on the main channel are provided after the fifth-order branch channel from the inlet. Regarding the larger flow resistance on the branch channels near the inlet so it needs flow restraint on the main channel after the long branch channel. The increase in baffle height in the main channel starts from 0.1 to 0.5 mm, with an increase of 0.1 mm after three baffles. The mother channel hydraulic diameter (d_m) for the inlet area calculated based on the hydraulic diameter of the branch channel (d_b) considering Murray's theory with equation (Fahruddin et al. 2019b):

$$d_m^3 = \Sigma d_b^3 \tag{1}$$

Table 2. Grid independency.

Mesh type	Mesh A	Mesh B	Mesh C	Mesh D
Max face size (mm)	1.2	1.1	1	0.9
Cells	8360	11333	19788	24400
Faces	19906	26956	45569	55826
Nodes	3570	4842	7121	8521
Velocity magnitude (m/s)	1.303	1.325	1.308	1.315
Static pressure (Pa)	121.79	136.65	132.45	134.18
Velocity diff. (%)	0.90	0.81	0.50	0.00
Pressure diff. (%)	9.2	1.8	1.3	0.00

The data based on fuel cell performance obtained using experimental schematics as shown in Figure 3. Subsequently, the hydrogen and oxygen gas supplies are stored in pressurised tubes. The tube's pressure is then reduced using a regulator, and once it is sufficient, the Hydrogen and Oxygen flowrate is adjusted using a flowmeter. The hydrogen flow rate used was 0.15 slpm (standard litre per minute), while the oxygen flow rates are 0.4 slpm at 1 atm back pressure (Tafaoli et al. 2011).

Furthermore, to obtain appropriate humidity and temperature of the reactant, a humidifier was used in the hydrogen and oxygen gas lines before the cell and a cartridge heater was installed at the endplate. The cell temperature used was 50°C, and it is measured using a thermocouple placed on the endplate cell and connected to the thermocontrol, which turns on the cartridge heater when the temperature drops. Digital thermometer and pressure transducer with DAQ calibrated using alcohol thermometer and manometer, respectively, over data ranges according to operating conditions. The polarisation data were obtained using a Programmable DC Electronic Load DL3021. The polarisation curve is obtained by varied voltage from 0.2 to 0.9 V, with 0.1 V difference. The cell was run for 15 min under an open circuit to achieve stable conditions. And each loading step is maintained for 5 min to simulate the PEMFC loading process as fluctuating conditions in-vehicle operation (Huang, Zhao, and Jian 2019).

2.2. Numerical method

Numerical simulation is used to analyse flow characteristics. Numerical simulations were carried out using the Ansys Fluent student version to obtain the distribution of velocity and static pressure on the cathode flow field. A finer mesh will produce more accurate values but will take longer. Therefore, a grid independence test was carried out to obtain the optimal mesh density. In this study, several variations of mesh density were used by setting the maximum face size. The analysis showed that the maximum face size of 1 mm achieved optimal results, resulting in a total of 19,788 cells and 45,569 faces in the leaf flow field. When compared with a denser mesh with a maximum face size of 0.9 mm, it was found that the maximum difference in velocity magnitude and static pressure was less than 1.5% as shown in Table 2. The boundary condition is set as the inlet mass flow of 2.0.10^{-5} kg/s. The operating pressure and temperature are 1 atm and 60°C, respectively. The governing equation used is expressed as (Lakshminarayanan et al. 2019):

Continuity equation

$$\frac{\partial \rho}{\partial t} + \nabla.(\partial v) = 0 \tag{2}$$

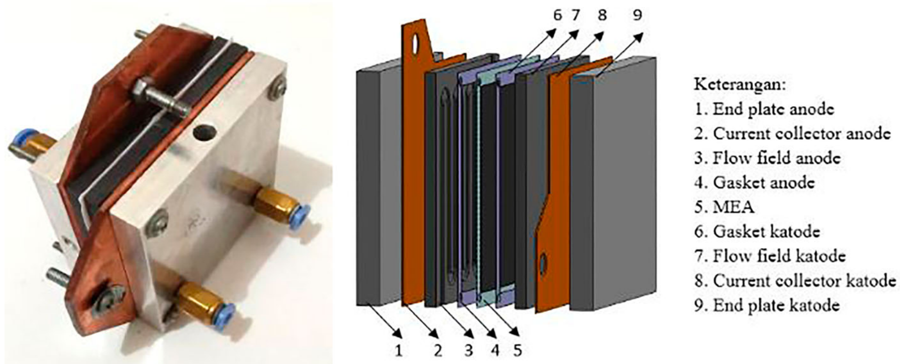

Figure 1. PEM *fuel cell* configuration.

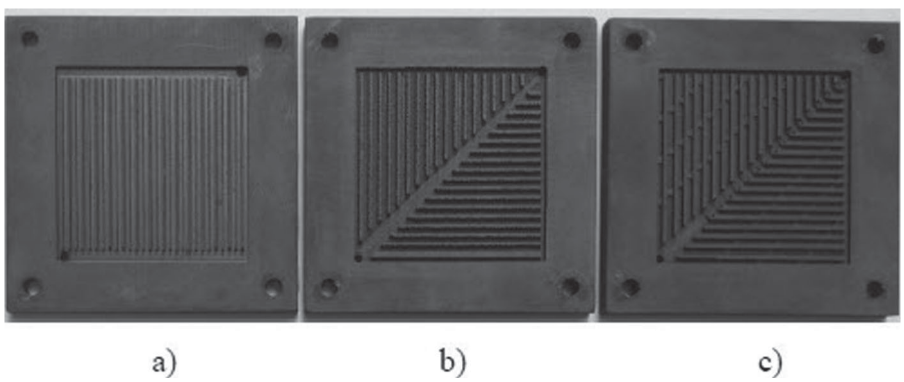

Figure 2. Cathode flow field variation: (a) parallel, (b) leaf, (c) leaf-baffle.

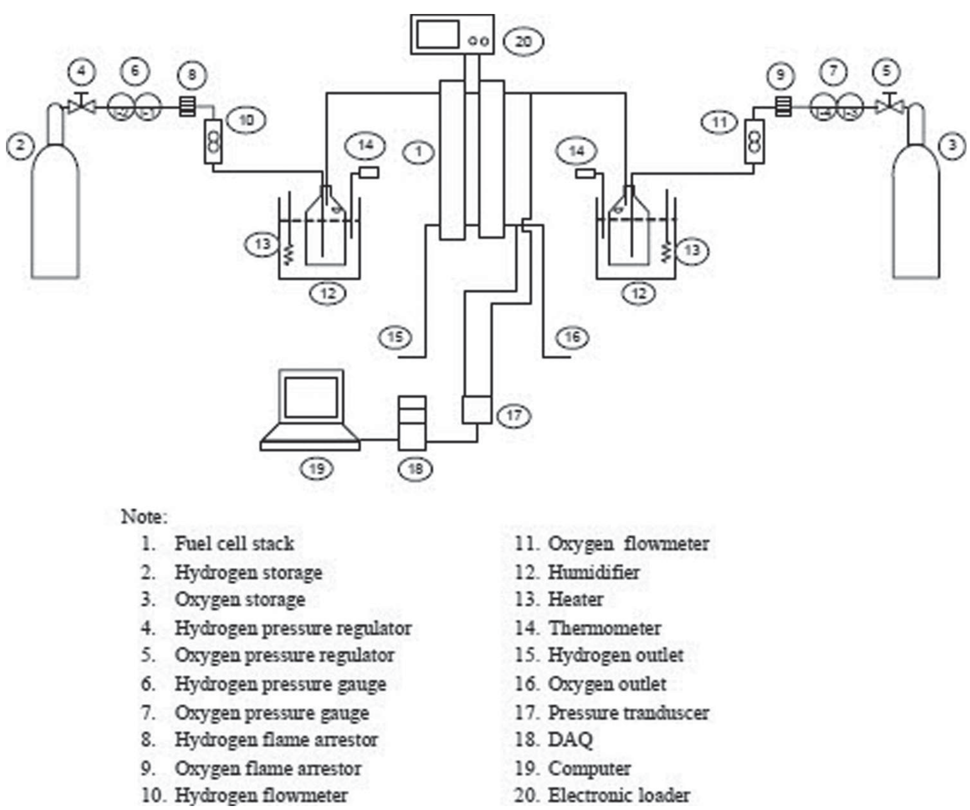

Figure 3. Experimental installation.

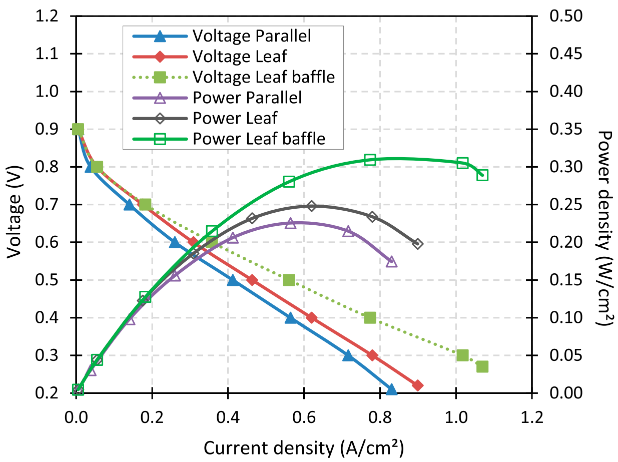

Figure 4. The effect of flow field design on current density and power density.

Conservation of momentum

$$\frac{\partial(\rho v)}{\partial t} + \nabla.(\rho vv) = -\nabla\rho + \nabla.(\mu_{\text{eff}}\nabla v) + Sm \quad (3)$$

Uniformity index (γ) was calculated to determine the velocity uniformity based on the average velocity ($\bar{u}$) and the area (A) (Nassau and Agarwal 2018):

$$\gamma = 1 - \int \frac{\sqrt{(\bar{u} - u)^2}}{2 \cdot A \cdot \bar{u}} dA \quad (4)$$

3. Results and discussion

3.1. The effect of cathode flow field variations on current density and power density

The use of a leaf-baffle flow field increases the reactants' pressure on the membrane and the layer of the catalyst, thereby boosting its supply to produce a larger current. The distribution of reactants in the leaf flow fields produces better uniformity than the parallel types. The addition of baffles in the main channel tends to enhance reactants' supply till the tip of the branch. Therefore, the distribution of reactants in the leaf-baffle flow field is better than in those lacking baffles. This is also consistent with the results of the simulation (Fahruddin et al. 2020). According to Figure 4, the use of a leaf-baffle flow field on the cathode generated a maximum current density of 1.070 A/cm^2 at a voltage of 0.27 V at 0.4 slpm. Furthermore, the use of a leaf and parallel flow fields produces a current density of 0.899 A/cm^2 at a voltage of 0.22 V and 0.831 A/cm^2 at a voltage of 0.21 V, respectively. The maximum power density that is achieved using a leaf-baffle flow field is 0.309 W/cm^2 at an electric voltage of 0.4 V. Furthermore, the leaf and parallel flow fields produce a power density of 0.248 and 0.226 W/cm^2, respectively at a similar voltage.

From Figure 4 can be seen that at low currents, the leaf polarisation graph coincides with the leaf-baffle polarisation graph. This shows that the ohmic losses in the leaf and leaf-baffle are close, because the surface of the leaf-baffle flow field in contact with the gas diffusion layer is identical to the leaf flow field. Compared to parallel flow fields, leaf flow fields have more channels. But when viewed on one axis, parallel flow fields have more channels. Therefore, with the same channel width, parallel flow fields have slightly narrower ribs so that the electrical resistance is slightly larger. At high currents, the leaf-baffle polarisation graph moves away from the leaf polarisation graph. This shows that the concentration losses in the leaf-baffle are smaller than the leaf flow field. And shows that the supply of reactants in the leaf-baffle is more well distributed. So that the cell with leaf-baffle produces a very good power density when compared to leaf and parallel flow fields.

Table 3. The improvement performance in accordance with flow field design variation.

	Compared to parallel		Compared to leaf
	Leaf	Leaf-baffle	Leaf-baffle
Current density max.	8.25%	28.80%	18.98%
Power density max.	9.93%	37.14%	24.75%

3.2. Increasing current and power densities by modifying the cathode flow field

Table 3 shows that the maximum current density produced by the leaf flow field is 8.25% greater than the parallel type. Furthermore, the use of a leaf-baffle flow field increases the current density by 28.8% when compared to the parallel type. And the current density with the leaf-baffle flow field is 18.98% greater than using the leaf flow field.

This is similar to the power density generated. The leaf-baffle flow field produced the maximum power density, which is approximately 24.75% and 37.14% higher than the leaf and parallel types respectively. The use of baffles leads to a significant increase in the current and power densities when compared to those without baffles, as reported in a study carried out by Heidary et al. (2016). In addition to increasing the pressure of the reactants towards the diffusion layer, baffles' use ensures it divides the flow towards the branches, thereby boosting its distribution in the field.

3.3. The effect of variation in oxygen flowrate on current density and power density

According to Figure 5, an increase in the cathode oxygen flow causes an increase in the current density. The maximum current density produced by the leaf-baffle flow field at a flow rate of 0.8 slpm is 1.097 A/cm^2 at 0.28 V. Furthermore, at a flow rate of 0.6 slpm, the maximum current density produced is 1.090 A/cm^2 at 0.278 V, while at a flow rate of 0.4 slpm it produces 1.070 A/cm^2 at 0.27 V. The greater the flow rate, the higher the reactant supply, and the higher the current density. However, excessive flow rate reduces the retention time of oxygen to the GDL, causing a short electrochemical reaction. Furthermore, when the flow rate is 0.8 slpm, a higher voltage can be achieved at the same current density because the reactants that accumulate at the cathode tend to increase the electric potential. According to the equation $= V_{\text{output}}/1.481$ V (Spiegel 2007), the efficiency of a hydrogen fuel cell depends on the voltage generated. In addition, in the use of leaf-baffles, the flow rate will increase the pressure of the reactants towards the diffusion

Table 4. Maximum net power with flow field variation.

Flow field	Power density (W/m^2)	Power (W)	Pressure drop (Pa)	Req.power (W)	Net power (W)
Parallel	0.226	5.6500	48.10	0.0003207	5.6497
Leaf	0.248	6.2000	37.10	0.0002473	6.1998
Leaf-baffle	0.309	7.7250	55.63	0.0003709	7.7246

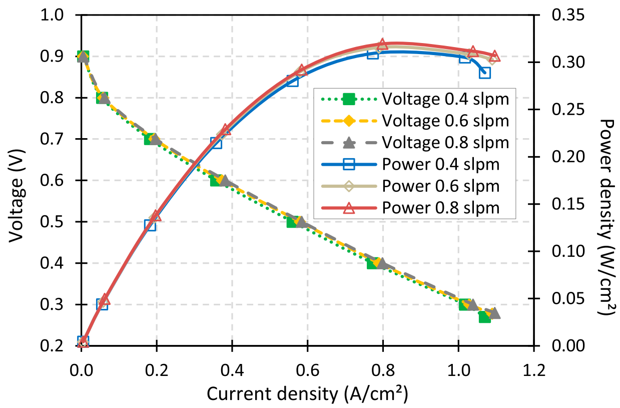

Figure 5. The effect of oxygen flow rate on current density and power density in the leaf-baffle flow field.

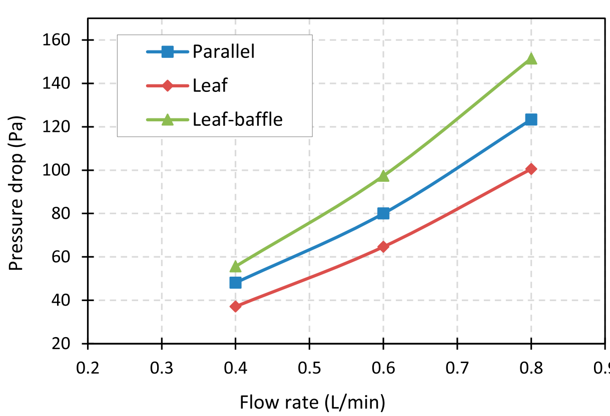

Figure 6. The effect of oxygen flow rate on pressure drop.

layer and increase the baffle turbulence. Therefore, it is theoretically reported that the higher the oxygen flow rate, the better the fuel cell efficiency, with sufficient retention time. At a flow rate of 0.8 slpm, the highest current density is achieved, resulting in a maximum power density of 0.319 W/cm^2 at 0.4 volts. At the same voltage, with oxygen flow rates of 0.6 and 0.4 slpm, the power density is 0.316 and 0.309 W/cm^2, respectively.

3.4. *Pressure drop and net power output*

Figure 6 shows that the higher the flow rate in all flow field designs, the higher the pressure drop. This is in accordance with the resistance theory of laminar flow through the channel, where major and minor losses are directly proportional to fluid velocity. The leaf flow field shows the least pressure drop compared to leaf-baffle or parallel types. Leaf also produces a less pressure drop than the parallel type because it has a blunt turn to the branching. While in the parallel flow field, the channel forms 90 degrees turning angle.

Meanwhile, the leaf-baffle flow field generates the greatest pressure compared to other variations. This is because the use of baffles in the primary and branch channels obstructs its flow. At a flow rate of 0.8 slpm, the pressure drop in a leaf-baffle flow field reaches 151.5 Pa, while in a leaf flow field, it generates 100.5 Pa. This simply means that the use of baffles increases the pressure drop by 50.75%. Table 4 shows the comparison of the maximum net power in accordance with the variation of the flow field designs. The additional force needed contra the pressure drop is relatively small compared to the output power generated by the fuel cell. This is because the flow rate of the reactants is quite slow. Where the power required to overcome the pressure drop is calculated from the flow rate times the pressure drop.

Although the use of baffles increases the pressure drop by 50.75% compared to leaf flow fields, it generated the best net power compared to the parallel and leaf without baffles. However, in a multi-stack fuel cell with a lot number of cells, it is necessary to pay attention to the additional power required to overcome the pressure drop in order to ensure the reactants in the last cell exert enough pressure to the diffusion layer (Velisala, Naga Srinivasulu, and Velisala 2018). On a single cell, the additional power required to overcome this pressure drop is only 0.0048% of the output power. Where the power required to overcome the pressure drop 55.63 Pa with 0.4 slpm flow rate is equal to 0.00037 W. Much smaller than the power generated by the cell of 7.72 W.

3.5. *Velocity and pressure distribution analysis with numerical simulation*

Numerically, from Table 5, it can be seen the comparison of values and uniformity index for the average velocity and static pressure of the reactants on the cathode side with parallel, leaf, and leaf-baffle flow fields. In general, the uniformity index in the parallel flow field is still better than in the leaf flow field. However, the average velocity in the leaf flow field is higher than in the parallel flow field. This is due to the occurrence of a special path in the parallel flow field so that in most channels in the parallel flow field the rate of reactants is slower. The greater the average velocity of the reactants in the leaf flow field is also followed by the greater the average static pressure when compared to the parallel flow field. The higher average velocity and pressure of the reactants results in a more adequate supply of reactants for

Table 5. Numerical simulation result data.

Term	Parallel	Leaf	Leaf-baffle
Uniformity index area-wt			
Velocity magnitude	0.5533	0.4750	0.5099
Static pressure	0.9135	0.9108	0.8980
Area-weighted average			
Velocity magnitude (m/s)	1.293	1.308	1.405
Static pressure (kPa)	0.1275	0.1321	0.1530

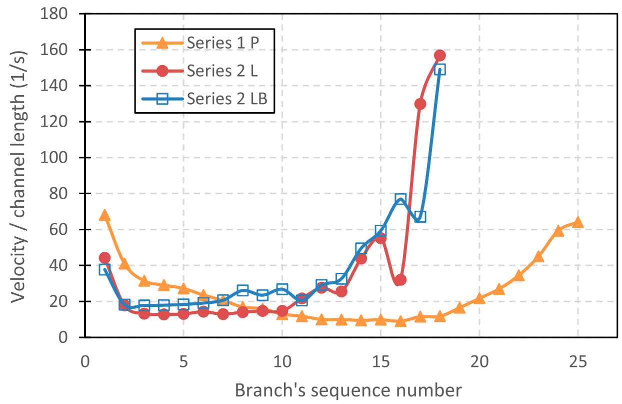

Figure 7. Comparison of branch entry velocity/channel length with flow field variations.

the entire reaction area, which results in a better current density. The use of baffles in the leaf flow field can increase the uniformity and the average velocity of the reactants. So that the use of baffles will further increase the performance potential for leaf flow fields. However, the use of baffles causes a slight decrease in pressure uniformity, this is because the pressure towards the diffusion layer at the points where the baffles are located will be greater.

Figure 7 shows the ratio of the velocity of the reactants entering the branch compared to the length of the channel for each branch's sequence number from the inlet. To provide an adequate supply of the reaction, the amount of reactants entering the branch must be proportional to the length of the branch. Because the longer the branch will require more reactant, so there is no void reaction at the end of the branch. Figure 7 shows that the leaf flow field has an advantage over parallel, where branch's sequence number nine and above have a better ratio. Need to remember that the branches close to the outlet require a larger reactant velocity because the oxygen concentration has decreased. Meanwhile, the leaf-baffle flow field shows the best velocity/channel length ratio.

When compared without baffles, the use of baffles in the leaf flow field can increase the velocity uniformity index. Although the value is still lower than the velocity uniformity index in the parallel flow field (Table 5). However, the leaf flow field provides a better average velocity/channel length ratio on the branch channel compared to parallel, so it can be said that the leaf flow field provides a better distribution of reactants as needed. The use of baffles in the leaf flow field gives an even better velocity/channel length ratio, because the reactants are slightly forced towards the longer branches (Figure 7). In the downstream flow area, the branches are shorter, thus requiring less reactant supply. A more proportional distribution of reactants at each point will give a better current value according to the Buttler-Volmer equation. However, studies on current distribution need to be investigated further with a focus on the profile of electrochemical activity and thus the durability of the cell.

4. Conclusion

Based on this study, it was known that the use of a leaf flow field on the cathode significantly increases the current and power densities when compared to the parallel type. The addition of baffles in the leaf flow field improves the performance of the fuel cell for the better. It increases the current and power densities by 18.98% and 24.75%, respectively, compared to without baffles. The use of baffles allows for a better distribution of reactants, providing better velocity for branch channels according to their length. The leaf flow field with baffles produces a higher pressure drop by 50.75% when compared to without baffles, at a flow rate of 0.4 slpm. However, compared to the electric power generated, the pump power used to overcome the pressure drop is very small, hardly affects the net power of a single cell. Further studies need to be carried out on fuel cells with multiple cells.

Acknowledgements

The authors gratefully acknowledge doctoral scholarship from Lembaga Pengelola Dana Pendidikan (LPDP) Ministry of Finance of Republic of Indonesia to A'rasy Fahruddin, and facility support from the Direktorat Riset dan Pengabdian kepada Masyarakat (DRPM) and Department of Mechanical Engineering Institut Teknologi Sepuluh Nopember (ITS) Indonesia.

Disclosure statement

No potential conflict of interest was reported by the author(s).

Funding

The authors gratefully acknowledge doctoral scholarship from Lembaga Pengelola Dana Pendidikan (LPDP), Ministry of Finance of Republic of Indonesia to A'rasy Fahruddin.

ORCID

A'rasy Fahruddin http://orcid.org/0000-0003-1986-4936

References

Arat, Hüseyin Turan, Meryem Gizem Sürer, Semir Gökpinar, and Kadir Aydin. 2020. "Conceptual Design Analysis for a Lightweight Aircraft with a Fuel Cell Hybrid Propulsion System." *Energy Sources, Part A: Recovery, Utilization and Environmental Effects*. doi:10.1080/15567036.2020.1773966.

Badduri, Srinivasa Reddy, G. Naga Srinivasulu, and S. Srinivasa Rao. 2019. "Experimental Analysis of PEM Fuel Cell Performance Using Lung Channel Design Bipolar Plate." *International Journal of Green Energy* 16 (15): 1591–1601. doi:10.1080/15435075.2019.1677238.

Bhatia, Krishan Kumar, and William T Riddell. 2016. "Identifying and Modeling Key Trade-Offs Between Hydrogen Fuel Cell and Electric Vehicles." *International Journal of Sustainable Engineering* 9 (3): 215–222. doi:10.1080/19397038.2015.1128494.

Cordiner, S., V. Mulone, A. Giordani, M. Savino, G. Tomarchio, T. Malkow, G. Tsotridis, A. Pilenga, M. L. Karlsen, and J. Jensen. 2016. "Fuel Cell Based Hybrid Renewable Energy Systems for Off-Grid Telecom Stations: Data Analysis from on Field Demonstration Tests Q." *Applied Energy*. doi:10.1016/j.apenergy.2016.08.162.

Demirbas, A. 2007. "Fuel Cells as Clean Energy Converters." *Energy Sources, Part A: Recovery, Utilization, and Environmental Effects* 29 (2): 185–191. doi:10.1080/009083190948694.

Demirbas, A. 2009. "Biofuel Fueled Cell Applications." *Energy Sources, Part A: Recovery, Utilization, and Environmental Effects* 32 (1): 36–44. doi:10.1080/15567030802464370.

Fahruddin, A'rasy, Djatmiko Ichsani, Fadlilatul Taufany, and Budi Utomo Kukuh Widodo. 2019a. "The Effect of Channel Width on Biometric Flow Field Towards Performance of Polymer Electrolyte Membrane Fuel Cell." *Journal of Engineering Science and Technology* 14 (5): 2552–2564.

Fahruddin, A., D. Ichsani, F. Taufany, and B. U. K. Widodo. 2019b. "The Effect of Mother Channel Width on Biometric Flow Field Towards Polymer Electrolyte Membrane Fuel Cell Performance." *Journal of Physics: Conference Series* 1402: 4. doi:10.1088/1742-6596/1402/4/044042.

Fahruddin, Arasy, Djatmiko Ichsani, Fadlilatul Taufany, Budi U. K. Widodo, and Wawan A. Widodo. 2020. "The Effect of Baffle Shape on the Performance of a Polymer Electrolyte Membrane Fuel Cell with a Biometric Flow Field." *International Journal of Hydrogen Energy*. doi:10.1016/j.ijhydene.2020.08.054.

Heidary, Hadi, Mohammad J Kermani, Suresh G Advani, and Ajay K Prasad. 2016. "Experimental Investigation of In-Line and Staggered Blockages in Parallel Flowfield Channels of PEM Fuel Cells." *International Journal of Hydrogen Energy* 41 (16): 6885–6893. doi:10.1016/j.ijhydene.2016.03.028.

Hosseini, Seyed Ehsan, and Brayden Butler. 2020. "An Overview of Development and Challenges in Hydrogen Powered Vehicles." *International Journal of Green Energy* 17 (1): 13–37. doi:10.1080/15435075.2019.1685999.

Hosseinzadeh, Elham, and Masoud Rokni. 2013. "Development and Validation of a Simple Analytical Model of the Proton Exchange Membrane Fuel Cell (PEMFC) in a Fork-Lift Truck Power System." *International Journal of Green Energy* 10 (5): 523–543. doi:10.1080/15435075.2012.678525.

Huang, Zipeng, Jing Zhao, and Qifei Jian. 2019. "Voltage Behavior Improvement for Proton Exchange Membrane Fuel Cell Stack Suffering Fuel Starvation." *Energy Sources, Part A: Recovery, Utilization, and Environmental Effects*. doi:10.1080/15567036.2019.1674962.

Inal, Omer Berkehan, and Cengiz Deniz. 2020. "Assessment of Fuel Cell Types for Ships: Based on Multi-Criteria Decision Analysis." *Journal of Cleaner Production* 265: 121734. doi:10.1016/j.jclepro.2020.121734.

Kloess, Jason P., Xia Wang, Joan Liu, Zhongying Shi, and Laila Guessous. 2009. "Investigation of Bio-Inspired Flow Channel Designs for Bipolar Plates in Proton Exchange Membrane Fuel Cells." *Journal of Power Sources* 188 (1): 132–140. doi:10.1016/j.jpowsour.2008.11.123.

Lakshminarayanan, V., and P. Karthikeyan. 2020. "Performance Enhancement of Interdigitated Flow Channel of PEMFC by Scaling up Study." *Energy Sources, Part A: Recovery, Utilization, and Environmental Effects* 42 (14): 1785–1796. doi:10.1080/15567036.2019.1604889.

Lakshminarayanan, V., K. Niveda, S. Akash, and P. Anand. 2019. "Numerical Analysis for Two Pass Interdigitated Flow Channel of PEMFC." *International Journal of Ambient Energy* 42 (8): 907–911. doi:10.1080/01430750.2019.1568911.

Lim, B. H., E. H. Majlan, W. R. W. Daud, T. Husaini, and M. I. Rosli. 2016. "Effects of Flow Field Design on Water Management and Reactant Distribution in PEMFC: A Review." *Ionics* 22: 301–316. doi:10.1007/s11581-016-1644-y.

Liu, Zhenling. 2019. "Experimental Analysis of an Integrated Biomass Gasification and PEM Fuel Cell System." *Energy Sources, Part A: Recovery, Utilization, and Environmental Effects* 41 (3): 360–367. doi:10.1080/15567036.2018.1518354.

Lu, Jun, Tian Tang, Chao Bai, Huizhong Gao, Junguang Wang, Cheng Li, Yuke Gao, Zhaoyuan Guo, and Xiao Zong. 2020. "Reviews of Fuel Cells and Energy Storage Systems for Unmanned Undersea Vehicles." *Energy Sources, Part A: Recovery, Utilization and Environmental Effects*. doi:10.1080/15567036.2020.1795313.

Manso, A. P., F. F. Marzo, J. Barranco, X. Garikano, and M. Garmendia Mujika. 2012. "Influence of Geometric Parameters of the Flow Fields on the Performance of a PEM Fuel Cell. A Review." *International Journal of Hydrogen Energy* 37 (20): 15256–15287. doi:10.1016/j.ijhydene.2012.07.076.

Nassau, Christopher J., and Ramesh K. Agarwal. 2018. "Curvature Effects and Flow Uniformity Optimization of a Blood Microchannel." *Mechanical Engineering and Materials Science Independent Study* 71. https://openscholarship.wustl.edu/mems500/71.

Ozden, Adnan, Mustafa Ercelik, David Ouellette, C. Ozgur Colpan, Hadi Ganjehsarabi, and Feridun Hamdullahpur. 2017. "Designing, Modeling and Performance Investigation of Bio-Inspired Flow Field Based DMFCs." *International Journal of Hydrogen Energy* 42 (33): 21546–21558. doi:10.1016/j.ijhydene.2017.01.007.

Pan, Mingzhang, Xianpan Meng, Chao Li, Jinyang Liao, and Chengjie Pan. 2020. "Impact of Nonuniform Reactant Flow Rate on the Performance of Proton Exchange Membrane Fuel Cell Stacks." *International Journal of Green Energy* 17 (11): 603–616. doi:10.1080/15435075.2020.1761812.

Roshandel, R., F. Arbabi, and G. Karimi Moghaddam. 2012. "Simulation of an Innovative Flow-Field Design Based on a Bio Inspired Pattern for PEM Fuel Cells." *Renewable Energy* 41: 86–95. doi:10.1016/j.renene.2011.10.008.

Sarma, Upasana, and Sanjib Ganguly. 2018. "Determination of the Component Sizing for the PEM Fuel Cell-Battery Hybrid Energy System for Locomotive Application Using Particle Swarm Optimization." *Journal of Energy Storage* 19 (February): 247–259. doi:10.1016/j.est.2018.08.008.

Spiegel, Colleen. 2007. *Designing and Building Fuel Cells*. New York City: McGraw-Hill Professional.

Stempien, J. P., and S. H. Chan. 2017. "Comparative Study of Fuel Cell, Battery and Hybrid Buses for Renewable Energy Constrained Areas." *Journal of Power Sources* 340: 347–355. doi:10.1016/j.jpowsour.2016.11.089.

Tafaoli, Masoule M., M. Shakeri, Q. Esmaili, and A. Bahrami. 2011. "PEM Fuel Cell Modeling and Pressure Investigation." *Energy Sources, Part A: Recovery, Utilization, and Environmental Effects* 33 (24): 2291–2302. doi:10.1080/15567030903530566.

Velisala, Venkateswarlu, and Naga Srinivasulu Golagani. 2020. "Computational Fluid Dynamics Study of Serpentine Flow Field Proton Exchange Membrane Fuel Cell Performance." *Heat Transfer Engineering* 41 (6–7): 650–664. doi:10.1080/01457632.2018.1546975.

Velisala, Venkateswarlu, G Naga Srinivasulu, and Venkateswarlu Velisala. 2018. "Computational Fluid Dynamics Study of 3-Pass Serpentine Flow Field Configuration on Proton Exchange Membrane Fuel Cell Performance." *International Journal of Ambient Energy* 41 (2): 183–188. doi:10.1080/01430750.2018.1456959.

Wang, Jinshi, Junjie Yan, Jinliang Yuan, and Bengt Sundén. 2011. "On Flow Maldistribution in PEMFC Stacks." *International Journal of Green Energy* 8 (5): 585–606. doi:10.1080/15435075.2011.576288.

Zhang, Guoqiang, Juan Zhang, and Tian Xie. 2020. "A Solution to Renewable Hydrogen Economy for Fuel Cell Buses A Case Study for Zhangjiakou in North." *International Journal of Hydrogen Energy* 45 (29): 14603–14613. doi:10.1016/j.ijhydene.2020.03.206.